INFECTION AND IMMUNITY, Mar. 2003, p. 1527–1537 Vol. 71, No. 3
0019-9567/03/$08.00+0 DOI: 10.1128/IAI.71.3.000–000.2003

Mutant *Escherichia coli* Heat-Labile Toxin B Subunit That Separates Toxoid-Mediated Signaling and Immunomodulatory Action from Trafficking and Delivery Functions

Sylvia A. Fraser,[1] Lolke de Haan,[1] Arron R. Hearn,[2] Heather K. Bone,[1] Robert J. Salmond,[1] A. Jennifer Rivett,[2] Neil A. Williams,[1] and Timothy R. Hirst[1]*

Departments of Pathology & Microbiology[1] and Biochemistry,[2] School of Medical Sciences, University of Bristol, University Walk, Bristol BS8 1TD, United Kingdom

Received 23 September 2002/Returned for modification 8 November 2002/Accepted 18 November 2002

The homopentameric B-subunit components of *Escherichia coli* heat-labile enterotoxin (EtxB) and cholera toxin (CtxB) possess the capacity to enter mammalian cells and to activate cell-signaling events in leukocytes that modulate immune cell function. Both properties have been attributed to the ability of the B subunits to bind to GM1-ganglioside receptors, a ubiquitous glycosphingolipid found in the plasma membrane. Here we describe the properties of EtxB(H57S), a mutant B subunit with a His→Ser substitution at position 57. The mutant was found to be severely defective in inducing leukocyte signaling, as shown by failure to (i) trigger caspase 3-mediated $CD8^+$-T-cell apoptosis, (ii) activate nuclear translocation of NF-κB in Jurkat T cells, (iii) induce a potent anti-B-subunit response in mice, or (iv) serve as a mucosal adjuvant. However, its GM1 binding, cellular uptake, and delivery functions remained intact. This was further validated by the finding that EtxB(H57S) was as effective as EtxB in delivering a conjugated model class I epitope into the major histocompatibility complex class I pathway of a dendritic cell line. These observations imply that GM1 binding alone is not sufficient to trigger the signaling events responsible for the potent immunomodulatory properties of EtxB. Moreover, they demonstrate that its signaling properties play no role in EtxB uptake and trafficking. Thus, EtxB(H57S) represents a novel tool for evaluating the complex cellular interactions and signaling events occurring after receptor interaction, as well as offering an alternative means of delivering attached peptides in the absence of the potent immunomodulatory signals induced by wild-type B subunits.

Heat-labile enterotoxin from *Escherichia coli* (Etx) and its close homologue, cholera toxin (Ctx), from *Vibrio cholerae* are the primary virulence determinants responsible for causing traveller's diarrhea and cholera, respectively (reviewed in references 44 and 47). Both Etx and Ctx are heterohexameric molecules, comprised of a single A subunit and five identical B subunits. The toxin B subunits, EtxB and CtxB, respectively, play a critical role in toxin action by mediating high-affinity binding to GM1 ganglioside receptors on target cell surfaces. Such binding triggers toxin internalization into an endocytic retrograde trafficking pathway to the *trans*-Golgi network (reviewed in reference 23). The toxin A subunits are then thought to be translocated via the Sec61p channel of the endoplasmic reticulum (ER) into the cytosolic compartment of the cell, where they irreversibly ADP-ribosylate $G_{s\alpha}$, a regulatory subunit of the adenylate cyclase complex. This leads to enhanced intracellular cyclic AMP levels, increased Cl^- secretion, inhibition of Na^+ adsorption, and, eventually, the osmotic movement of a large quantity of water into the intestinal lumen and concomitant diarrhea.

In addition to serving as delivery vehicles, Etx and Ctx have been found to possess remarkable immunomodulatory properties. Evidence has accumulated which shows that both A- and B-subunits have distinct immunomodulatory activities that act synergistically, provoking a potent antitoxin response and substantially augmenting immune responses to coadministered antigens (10, 36, 55). Recombinant preparations of the B subunits devoid of contaminating A subunits are also highly immunogenic upon systemic and mucosal immunization; and EtxB, and to a lesser extent, CtxB, can act as mucosal adjuvants to coadministered unrelated antigens (12, 14, 25, 30, 32, 37, 51, 54, 59). In addition, EtxB and CtxB have been shown to be able to modulate T-helper 1 (Th1)-type responses associated with inflammatory autoimmune disorders such as arthritis, diabetes, and multiple sclerosis (4, 48, 56). Several studies have indicated that GM1 binding plays a critical role in B-subunit-mediated immunomodulation, and a GM1-binding mutant, EtxB(G33D), containing a Gly33→Asp substitution, was found to lack the immunogenic, immunomodulatory, and adjuvant properties of the native B subunit (11, 32, 56). However, the mechanisms which underlie the remarkable immunomodulatory properties of these molecules have yet to be fully resolved.

A potential explanation for the immunomodulatory activities of EtxB and CtxB involves their marked effects on the differentiation and survival of leukocytes. In this respect, EtxB and CtxB have been found to (i) affect antigen processing and presentation by macrophages (8, 27, 29), (ii) induce cytokine secretion by monocytes (53), (iii) stimulate the proliferation of B and $CD4^+$ T cells (5, 16, 24, 31, 52, 58), and (iv) induce apoptosis in $CD8^+$ T cells (33, 52, 60). For all of these effects a role for GM1 binding has been implicated. This suggests that B-subunit-mediated cross-linking of GM1 receptors on leukocytes leads to activation of intracellular signaling pathways that

* Corresponding author. Mailing address: Department of Pathology & Microbiology, University of Bristol, School of Medical Sciences, University Walk, Bristol BS8 1TD, United Kingdom. Phone: 44-117-9287538. Fax: 44-117-9300543. E-mail: t.r.hirst@bristol.ac.uk.

influence leukocyte differentiation. Indeed, our recent studies have shown that EtxB-mediated induction of apoptosis in $CD8^+$ T cells is dependent on the activation of the transcription factors NF-κB and Myc, and both caspase 3 and 8 (42, 46). Furthermore, we found that EtxB-mediated up-regulation of major histocompatibility complex class II (MHC-II) and CD25 cell surface expression on B cells is dependent on signaling pathways activated through P-I-3 kinase (5). Importantly, EtxB(G33D) failed to activate these signaling pathways, indicating that receptor interaction is crucial (5, 42, 46). As a consequence, we postulated that B subunit-GM1 interaction is responsible for the activation of signaling events that lead to immunomodulation (55).

Interestingly, we recently reported the generation of a CtxB mutant, CtxB(H57A), that retained the ability to bind with high affinity to GM1 and yet was severely defective as an immunomodulator (1). CtxB(H57A) was found to be unable to trigger $CD8^+$-T-cell apoptosis, upregulate CD25 expression on B cells, or stimulate a significant anti-B subunit response in vivo. X-ray crystallographic analysis of CtxB(H57A) revealed that the His57→Ala substitution caused a striking 7-Å shift in the position of an exposed loop adjacent to the GM1-binding pocket towards the central pore of the molecule (1). Even though this loop, comprising amino acids 52 to 58, is adjacent to the receptor-binding pocket, the His57 mutation did not significantly alter the position of the amino acid residues involved in GM1 binding or interfere with the capacity of the molecule to cocrystallize with D-galactose (1). These unexpected findings indicate that GM1 binding alone is not sufficient to trigger the immunomodulatory properties of CtxB. Since this loop is fully conserved in EtxB, similar mutations within the loop might also be expected to result in a corresponding loss in immunomodulation. Here, we investigate the immunomodulatory properties of EtxB(H57S) (41) and, in addition, seek to establish whether the failure to activate signaling events in leukocytes affects the GM1-mediated pathway of B subunit internalization.

MATERIALS AND METHODS

Expression and purification of recombinant toxins. Plasmid pMMB68, which encodes wild-type EtxB; plasmid pTRH64, which encodes the non-GM1-binding EtxB(G33D), containing a Gly→Asp substitution at position 33; and plasmid pTRH75, which encodes EtxB(H57S), containing a His→Ser substitution at position 57, were constructed as reported earlier (2, 32, 41). In addition, plasmid pTRH78, which encodes EtxB(H57A), containing a His→Ala substitution at position 57, was generated by PCR mutagenesis (19). In brief, plasmid pTRH23 (61), a pBluescript IIKS derivative containing the *etxB* gene, was used as a PCR template, with the resultant mutant PCR fragment being cloned into the *Eco*RI-*Spe*I sites of pTRH23. The gene was sequenced by dideoxy sequencing (Molecular Recognition Centre, University of Bristol, Bristol, United Kingdom) and shown to encode EtxB with a single His→Ala substitution at position 57. The mutant *etxB*(H57A) allele was subcloned into the *Eco*RI-*Spe*I sites of pTRH64, and the resultant plasmid was designated pTRH78. Plasmids were electroporated into a nontoxigenic marine vibrio, *Vibrio* sp. strain 60, and EtxB, EtxB(G33D), EtxB(H57S), and EtxB(H57A) were expressed upon induction with isopropyl β-D-1-thiogalactopyranoside (IPTG) (Sigma, Poole, United Kingdom). Subsequently, recombinant proteins were purified using diafiltration, and hydrophobic interaction and ion-exchange chromatography as originally described by Amin et al. (2). Toxin pools were LPS-depleted using detoxi-gel columns (Pierce, Rockford, Ill), and contained ≤50 endotoxin units (EU) per mg protein, as determined in a *Limulus* amoebocyte lysate assay (BioWhittaker, Walkersville, Md.). Purified toxins were analyzed either boiled or unheated on sodium dodecyl sulfate (SDS)–12.5% polyacrylamide gels stained with Coomassie blue.

Fluorimetric analysis of GM1-binding by recombinant toxins. The emission spectra of EtxB, EtxB(G33D), and EtxB(H57S) in the presence or absence of GM1 were recorded upon excitation at 280 nm, as described previously by De Wolf et al. (13). In brief, purified B subunit preparations were diluted in PBS (phosphate-buffered saline, pH 7.6, containing 0.5 M NaCl) to a final concentration of 50 μM and dispensed into 0.5-ml, 5-mm-path-length quartz cuvettes (StarnaBrand, Hainault, United Kingdom). The cuvettes were incubated for 5 min at 37°C in an LS50 spectrofluorimeter (Perkin-Elmer, Beaconsfield, United Kingdom) to equilibrate and then excited at 280 nm. Emission of fluorescence was recorded between 300 and 450 nm. Subsequently, a fivefold molar excess of GM1 was added to the cuvettes, and after mixing and incubation for 5 min at 37°C, the proteins were again excited at 280 nm and emission of fluorescence was recorded. Emission spectra presented were averaged over three scans.

GM1 ELISA. The capacity of EtxB, EtxB(G33D), and EtxB(H57S) to bind to GM1 was determined in a GM1 sandwich enzyme-linked immunosorbent assay (ELISA), essentially as described previously (2). In short, 96-well ELISA plates with high binding capacity (Dynatech, Alexandria, Va.) were coated overnight at 37°C with GM1 (1 μg/ml) in coating buffer (0.1 M NaH_2CO_3, 0.1 M $NaHCO_3$; pH 9.6 to 9.8), washed once with coating buffer, and then blocked with a 1% solution of skim milk powder (Marvel, Premier Brands, Moreton, United Kingdom) in coating buffer for 45 min at 37°C. After washing the plates with PBS, 1 μg of each B subunit diluted in PBS-Tween (PBS containing 0.05% Tween 20) was applied to the plate in duplicate wells and then serially diluted twofold in PBS-Tween and incubated for 1 h at 37°C. Subsequently, plates were washed with PBS-Tween and incubated with monoclonal antibody LDS16, specific for the EtxB pentamer (a kind gift from R. F. James, Department of Surgery, University of Leicester, Leicester, United Kingdom), diluted in PBS-Tween (1:1,500) and incubated for 1 h at 37°C. Plates were then washed with PBS-Tween and incubated with a horseradish peroxidase-conjugated goat antibody directed against mouse IgG (1:10,000) (Jackson ImmunoResearch Laboratories) for 1 h, 37°C, and then washed twice with PBS-Tween, and once with PBS. Bound B subunit was then detected by the addition of 50 mM phosphate buffer, pH 5.5, containing 0.02% *o*-phenylenediamine dihydrochloride (Sigma) and 0.006% perhydrol (Merck, Darmstadt, Germany). Plates were developed in the dark for 30 min at room temperature. After the addition of 50 μl of 2 M H_2SO_4 per well, absorbances were read at 492 nm (A_{492}) using an Anthos (Durham, N.C.) HTII ELISA reader and then plotted against the $\log_2$ of the dilution factor. The obtained results are expressed as the mean absorbance ± standard error of the mean (SEM).

Assessment of the binding of recombinant toxins to T cells. The capacity of recombinant EtxB, EtxB(G33D), and EtxB(H57S) to bind to $CD8^+$ or $CD4^+$ T cells isolated by magnetic cell-sorting columns from the mesenteric lymph node (MLN) of naive mice or to Jurkat T cells (43) was investigated by fluorescence-activated cell sorter (FACS) analysis, as described previously (33). Negatively selected $CD4^+$- and $CD8^+$-T-cell populations were >90% pure, as determined by flow cytometric analysis. For experiments involving the use of Jurkat T cells, cells were cultured to confluency in RP10 medium (RPMI 1640 containing Glutamax I, 100 μg of penicillin or streptomycin per ml, and 10% fetal bovine serum; all from GIBCO) at 37°C in a humidified CO_2 incubator and washed with PBS before use.

For the assessment of cell binding by the B subunits, purified $CD8^+$ or $CD4^+$ T cells or Jurkat T cells at a density of 2×10^6 cells/ml were incubated on ice with 100 nM wild-type or mutant B subunit for 1 h. Cells were then washed twice with ice-cold PBS and incubated with monoclonal antibody (MAb) 118-8 (1:500), specific for the EtxB pentamer (kindly provided by E. Lundgren and H. Persson, Department of Molecular Cell Biology, University of Umea, Umea, Sweden) for 30 min on ice. Subsequently, cells were washed with PBS and incubated with a fluorescein isothiocyanate (FITC)-labeled goat antibody specific for mouse immunoglobulin G (IgG) (1:500; Jackson ImmunoResearch Laboratories, West Grove, Pa.), 30 min on ice. Finally, cells were washed with FACS flow (Becton Dickinson, San Jose, Calif.), and analyzed by flow cytometry (FACScan; Becton Dickinson). PBS-treated cells were used as a control.

Apoptosis assays. The capacity of EtxB, EtxB(G33D), and EtxB(H57S) to deplete mixed MLN cell cultures from $CD8^+$ T cells was determined as described previously (33). Briefly, MLN cells were isolated from naive NIH mice as explained above and cultured for 48 h in modified Eagle's medium (GIBCO) in the presence of 100 nM wild-type or mutant B subunit. Incubation with PBS was used as a control. Cells were then washed and incubated with FITC-labeled CD4-specific and phycoerythrin-labeled CD8-specific antibodies (Pharmingen, San Diego, Calif.), and analyzed by flow cytometry.

To directly assess toxin-induced apoptosis of $CD8^+$ T cells, cell cycle analysis of toxin-treated $CD8^+$ T cells by propidium iodide staining was performed as previously described (33). In short, MLN $CD8^+$ T cells, negatively selected by

MACS, at 2×10^6 cells/ml were cultured for 15 h in the presence of EtxB, EtxB(H57S), or EtxB(H57A) at concentrations ranging from 1.5 nM to 1.0 μM in modified Eagle's medium supplemented with 20 mM HEPES, 4 mM L-glutamine, penicillin-streptomycin (each at 100 U/ml), 0.5 μM 2-mercaptoethanol, and 5% FBS. After incubation with the B subunits, cells were washed with Hanks balanced salt solution (HBSS), resuspended in 500 μl of HBSS containing 50 mM EDTA, and then permeabilized by the addition of 1 ml of ethanol. Cells were then washed twice with PBS and incubated in PBS containing propidium iodide (50 μg/ml) and RNase (40 μg/ml) (both from Sigma) for 1 h at room temperature. Following incubation, cells were washed once with PBS and then resuspended in FACS flow solution and analyzed by flow cytometry. The proportion of cells in the sub-G_0-G_1 stage of the cell cycle was then determined and plotted against the B-subunit concentration used.

Detection of caspase 3 activity in extracts of B-subunit-treated CD8$^+$ T cells. To determine B-subunit-mediated activation of caspase 3 activity, 3×10^6 purified MLN CD8$^+$ T cells were incubated with 100 nM EtxB, EtxB(G33D), or EtxB(H57S) for 18 h and then lysed in 50 mM HEPES buffer, pH 7.5, containing 50 mM KCl, 2 mM $MgCl_2$, 5 mM EDTA, 0.5 mM phenylmethylsulfonyl fluoride (PMSF), 1 mM dithiothreitol (DTT), 250 mM sucrose, 1% (vol/vol) NP-40, aprotinin (1 μg/ml), and leupeptin (1 μg/ml). Then, 25 μl of each lysate was added to 165 μl of 50 mM HEPES buffer, pH 7.4, containing 100 mM NaCl, 10 mM DTT, 1 mM EDTA, 0.1% (wt/vol) 3-[(cholamidopropyl)-dimethylammonio]-1-propanesulfonate (CHAPS), and 10% (vol/vol) glycerol. The reaction was then started by the addition of the artificial caspase 3 substrate Ac-Asp-Glu-Val-Asp-aminomethyl coumarin (Ac-DEVD-AMC) (Biomol Research Laboratories, Mamhead, United Kingdom) at a concentration of 25 μM. After incubation for 45 min at 37°C, the reaction was terminated by the addition of 100 μl of a solution containing 1% (wt/vol) sodium acetate and 200 mM acetic acid. AMC release was then determined by fluorimetry in an LS50 spectrofluorimeter (Perkin-Elmer), using an excitation wavelength of 380 nm and recording fluorescence emission at 460 nm. Fluorescence obtained with cell extracts from CD8$^+$ T cells treated with PBS was used as a control.

Detection of NF-κB activation by electrophoretic mobility shift assay. Activation of NF-κB by EtxB, EtxB(G33D), and EtxB(H57S) was investigated using a band shift assay, essentially as previously described (6). First, 10^7 Jurkat T cells were incubated with 100 nM wild-type or mutant B subunits for 2 h in RP10 medium. Incubation of cells with phorbol 12-myristate 13-acetate (PMA) (25 ng/ml; Sigma) and PBS was used as a positive and negative control, respectively. After 3 h, cells were harvested, washed with HBSS, and resuspended in 400 μl of 10 mM HEPES buffer, pH 7.9, containing 10 mM KCl, 1 mM Na_3VO_4, 10 mM NaF, 10 mM Na_2MoO_4, 1 mM DTT, 0.1 mM EDTA, 0.1 mM EGTA, 0.5 mM PMSF, aprotinin (2 μg/ml), leupeptin (1 μg/ml), pepstatin (1 μg/ml), 0.15 mM spermine, and 0.75 mM spermidine (all from Sigma). After incubation on ice for 15 min, (octylphenoxy)polyethoxyethanol (IGEPAL) (Sigma) was added to a final concentration of 0.3% (vol/vol), and the samples were vortexed and centrifuged to remove cytoplasmic proteins. Pelleted nuclei were then resuspended in 50 μl of 20 mM HEPES buffer, pH 7.9, containing 400 mM NaCl, 1 mM Na_3VO_4, 10 mM Na_2MoO_4, 10 mM NaF, 1 mM DTT, 1 mM EDTA, 1 mM EGTA, 0.5 mM PMSF, 25% glycerol, aprotinin (2 μg/ml), leupeptin (1 μg/ml), and pepstatin (1 μg/ml). After 15 min of agitation at 4°C, the samples were centrifuged and the supernatants, containing the extracted nuclear proteins, were transferred to a fresh vial and rapidly frozen by immersion in liquid nitrogen and then stored at −80°C.

To detect the presence of NF-κB in nuclear extracts, the protein content of each nuclear extract was determined using the Bio-Rad (Hemel Hempstead, United Kingdom) D_C protein assay, and the equivalent of 20 μg of total nuclear extract protein was incubated with 4×10^5 cpm of a [γ-^{32}P]ATP end-labeled oligonucleotide probe containing the binding sequence for NF-κB (5′-AGTTG AGGGGACTTTCCCAGGC-3′) in an 8.5 mM HEPES buffer, pH 7.5, containing 38 mM KCl, 0.6 mM $MgCl_2$, 1 mM DTT, 7.5% Ficoll, and 1 μg of poly(dI-dC) (Promega, Southampton, United Kingdom) for 20 min in a total volume of 20 μl. Samples were then subjected to gel electrophoresis on a 4% nondenaturing polyacrylamide gel at 150 V for 2 h. After electrophoresis, gels were dried and bound NF-κB was visualized by autoradiography.

Immunizations, sample collection, and ELISA. Groups of eight female NIH mice were immunized intranasally on day 0 with 10 μg of chicken egg albumin (OVA [grade V]; Sigma) alone, or admixed with either 10 μg of EtxB, EtxB(G33D), or EtxB(H57S). Mice received booster immunizations of the same composition on days 7 and 14. On day 21, animals were bled by cardiac puncture under ether anesthesia and then killed by cervical dislocation. OVA- and EtxB-specific serum IgG responses were then determined by ELISA, essentially as described above. In brief, plates were coated overnight with either EtxB (1 μg/ml) or OVA (1 μg/ml) in coating buffer, blocked, and then incubated with an appropriate dilution of serum of each individual mouse serially diluted twofold in PBS-Tween. Bound antibodies were detected using a horseradish peroxidase-conjugated goat antibody directed against mouse IgG (1:10,000) (Jackson ImmunoResearch Laboratories) and developed as described above. The observed OVA- and EtxB-specific antibody titers are given as the reciprocal of the calculated sample dilution corresponding with an A_{492} of ≥0.2. The results are expressed as the mean titer ± standard deviation for each group. Comparisons between experimental groups were made using Student's *t* test. Probability (*P*) values of <0.05 were considered significant.

Confocal microscopy. For microscopic analysis, 2×10^6 Jurkat T cells were incubated with 100 nM EtxB, EtxB(G33D), or EtxB(H57S) for 5 or 60 min at 37°C in 5% CO_2. Cells were then overlaid onto poly-L-lysine coated coverslips, fixed with 4% paraformaldehyde in PBS (vol/vol) for 10 min, and then permeabilized by incubation in 4% paraformaldehyde containing 0.5% Triton X-100 (Sigma) for 15 min. After repeated washing with PBS, cells were incubated with a polyclonal antiserum specific for EtxB (1:500; kindly provided by M. Pizza, IRIS, Chiron S.P.A., Siena, Italy) diluted in PBS-BSA (PBS containing 3% bovine serum albumin [fraction V, Sigma]) for 1 h at room temperature. Cells were then washed with PBS, and incubated with a FITC-labeled secondary antibody directed against rabbit IgG (1:100) (Jackson ImmunoResearch Laboratories) and tetramethyl rhodamine isothiocyanate (TRITC)-labeled wheat germ agglutinin (WGA) (Sigma) to visualize plasma and Golgi membranes (49). Washed coverslips were then mounted onto glass examination slides spotted with Mowiol containing 2.5% 1,4-diazabicyclo[2.2.2]octane (DABCO) antifading and 4′,6-diamidino-2-phenylindole dihydrochloride (DAPI) (1 mg/ml) for nuclear staining (all from Sigma). To demonstrate patch formation due to cross-linking of cell-bound toxin as described previously (5, 21), in separate experiments Jurkat T cells were sequentially incubated for 30 min at 4°C with EtxB, EtxB(G33D), or EtxB(H57S) and the EtxB-specific polyclonal antiserum (1:500). After an additional incubation period of 30 min at 37°C in 5%CO_2, cells were overlaid onto poly-L-lysine-coated coverslips and processed as described above. Coverslips were examined using a Leica (Buffalo, N.Y.) DH1RBE inverted confocal microscope at the MRC Cell Imaging Facility of the Department of Biochemistry, University of Bristol.

Antigen presentation assays. The capacity of EtxB, EtxB(G33D), EtxB(H57S), and EtxB(H57A) conjugates to deliver a 19-mer peptide containing the immunodominant OVA-derived SIINFEKL epitope into the MHC-I presentation pathway was investigated using a peptide conjugation and in vitro antigen presentation assay system described previously (9). In brief, toxin-peptide conjugates were prepared using the chemical bifunctional cross-linker *N*-(gamma-maleimido-butyryl-oxy) succinimide (GMBS) (Pierce). To this end, toxins were first reacted with GMBS in a 1:4 molar ratio, and GMBS-activated toxins were subsequently reacted with a 19-mer peptide (CAVGAGATAEESIINFEKL) at a 1:2 molar ratio. Toxin-peptide conjugates were then separated from excess peptide on a Sephadex G-50 column (Pharmacia, Uppsala, Sweden). To investigate if EtxB–, EtxB(G33D)–, and EtxB(H57S)–19-mer conjugates were capable of delivering the SIINFEKL epitope into the MHC-I antigen presentation pathway, conjugates were added to a 96-well plate, containing JAWSII dendritic cells (American Type Culture Collection, Manassas, Va.) seeded in RP10 medium at 2×10^5 cells/ml, at the peptide equivalent concentration of 100 nM. After 2 h of incubation with antigen, cells were fixed with 1% paraformaldehyde in PBS (vol/vol) for 10 min at room temperature, washed five times with RP10 medium containing 20 mM HEPES, 1 mM nonessential amino acids, 25 μM indomethacin, and amphotericin B (0.25 μg/ml) (all from GIBCO) and 50 μM 2-mercaptoethanol and then incubated overnight with RF33.70 T-cell hybridoma (38), recognizing the SIINFEKL peptide in the context of MHC-I at 5×10^5 cells/ml. In all experiments, equivalent concentrations of toxin admixed with 19-mer peptide and 19-mer peptide alone were also tested. Free 8-mer SIINFEKL peptide and PBS were used as a positive control and a negative control, respectively. After overnight incubation, presentation-induced interleukin-2 (IL-2) secretion by RF33.70 T-cell hybridoma was determined using a commercially available IL-2 ELISA kit (Pharmingen). IL-2 levels are given as mean units per milliliter ± SEM.

RESULTS

Characterization of the GM1- and cell-binding properties of EtxB(H57S). The EtxB(H57S) mutant was expressed in a marine vibrio, *Vibrio* sp. strain 60, and the secreted recombinant protein was purified by hydrophobic interaction and ion-exchange chromatography as described in Materials and Meth-

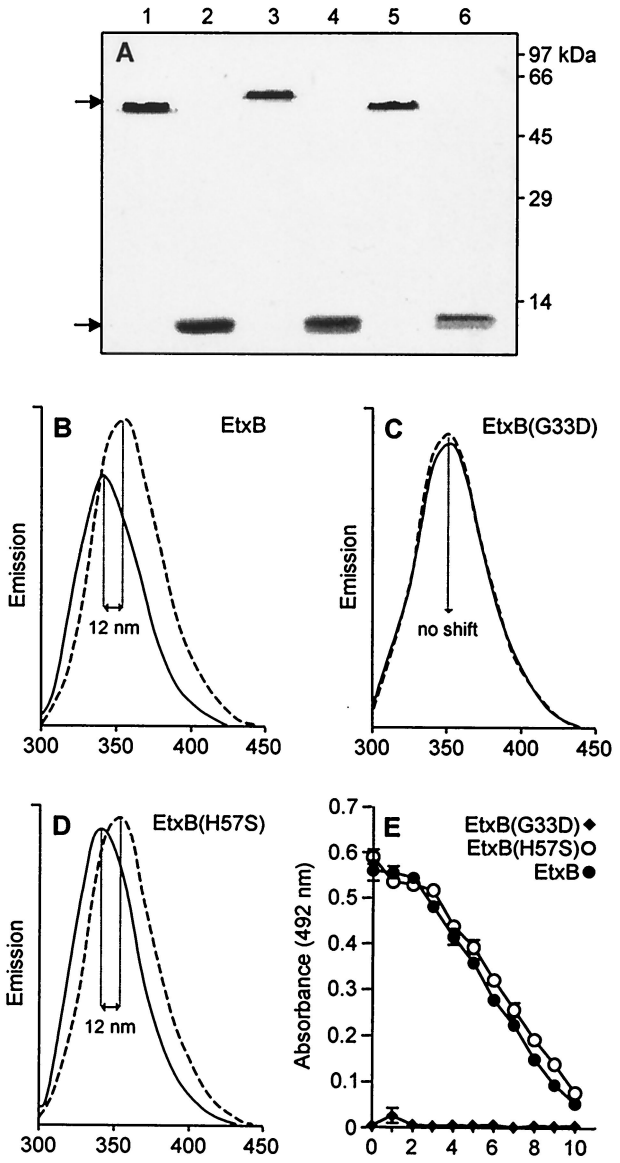

FIG. 1. Purification and characterization of the GM1-binding properties of EtxB, EtxB(G33D), and EtxB(H57S). (A) SDS-polyacrylamide gel electrophoresis analysis of EtxB, EtxB(G33D), and EtxB(H57S). Lanes: 1, EtxB unheated; 2, EtxB boiled; 3, EtxB(G33D), unheated; 4, EtxB(G33D), boiled; 5, EtxB(H57S), unheated; 6, EtxB(H57S), boiled. Molecular mass standards and EtxB monomer and pentamer (arrows) are indicated. (B to D) Analysis of Trp-fluorescence upon GM1 binding by EtxB, EtxB(G33D), and EtxB(H57S) by fluorescence spectroscopy. B-subunit preparations were diluted in quartz cuvettes to a final concentration of 5 μM in the presence (black curves) or absence (dashed curves) of a fivefold molar excess of GM1 and then left at 37°C for 5 min before excitation at 280 nm. Emission of fluorescence was then recorded between 300 and 450 nm. Emission spectra were averaged over three scans. The observed 12-nm blue shifts are indicated. (B) EtxB; (C) EtxB(G33D); (D) EtxB(H57S). (E) Analysis of the GM1-binding properties of EtxB, EtxB(G33D), and EtxB(H57S) by GM1 sandwich ELISA. GM1-coated plates were incubated with serial dilutions of EtxB, EtxB(H57S), or EtxB(G33D), and bound B subunit was subsequently detected using the EtxB pentamer-specific MAb LDS16, and a horseradish peroxidase-conjugated antibody specific for mouse IgG as described in Materials and Methods. Absorbances were read using an ELISA reader and are plotted against the $\log_2$ of the dilution factor. Data are given as mean ± SEM.

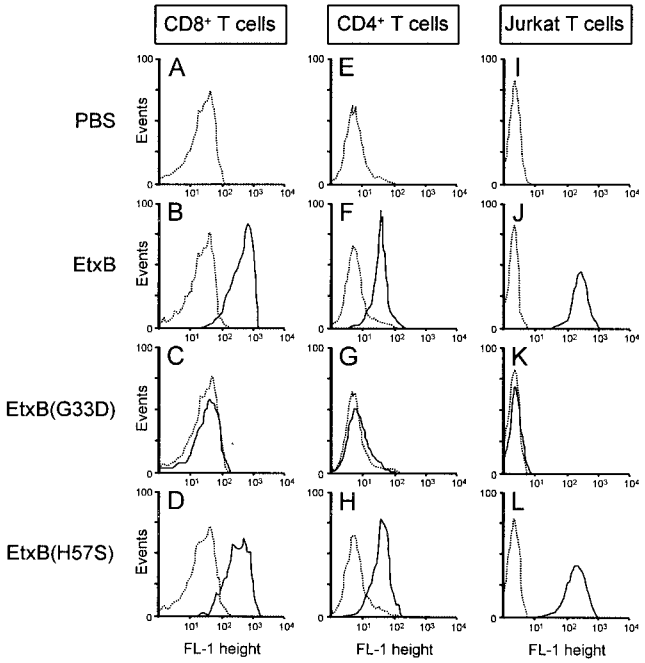

FIG. 2. EtxB(H57S) retains the ability to bind to $CD8^+$ cells, $CD4^+$ T cells, and Jurkat T cells. Cultured Jurkat T cells or $CD8^+$ T cells and $CD4^+$ T cells purified from the MLN of naive NIH mice as described in Materials and Methods were incubated on ice for 1 h in the absence or presence of 100 nM EtxB, EtxB(G33D), or EtxB(H57S). Cells were then sequentially incubated with the EtxB pentamer-specific MAb 118-8 and a FITC-labeled goat antibody specific for mouse IgG and analyzed by flow cytometry. Flow cytometric traces obtained with toxin-treated cells (black line) or PBS (dotted line) are shown. (A to D) $CD8^+$ T cells; (E to H) $CD4^+$ T cells; (I to L) Jurkat T cells.

ods. When applied to an SDS-polyacrylamide gel, EtxB(H57S) retained the characteristic stability properties of EtxB, migrating as a pentameric high-molecular-weight species if kept unheated prior to analysis (Fig. 1A, lanes 1 and 5) and dissociating into monomers when boiled (Fig. 1A, lanes 2 and 6). In agreement with our previous findings (11, 32), EtxB(G33D) behaved in a similar fashion, with the EtxB(G33D) pentamer migrating at a slightly slower electrophoretic mobility than the EtxB and EtxB(H57S) pentamers (Fig. 1A, compare lanes 1, 3, and 5) presumably due to the replacement of Gly33 with the negatively charged Asp residue. However, no difference in electrophoretic mobility was observed for the EtxB(G33D) monomer (Fig. 1A, lane 4). When the intrinsic pH stability of the EtxB(H57S) pentamer was tested as described previously by Ruddock et al. (40), it was found to possess pH stability characteristics similar to those of EtxB and EtxB(G33D), remaining pentameric at pH values as low as 1.6 (data not shown).

The GM1-binding capacity of EtxB(H57S) was first investigated by fluorescence spectroscopy using a method originally described by De Wolf et al. (13), which involves the detection of a 12-nm blue shift in the tryptophan emission spectrum upon B subunit-GM1 interaction. Accordingly, upon excitation at 280 nm the emission spectra of EtxB and EtxB(H57S) in the presence of a fivefold molar excess of GM1 exhibited a characteristic 12-nm blue shift in fluorescence (Fig. 1B and D). By contrast, EtxB(G33D), which had previously been shown to

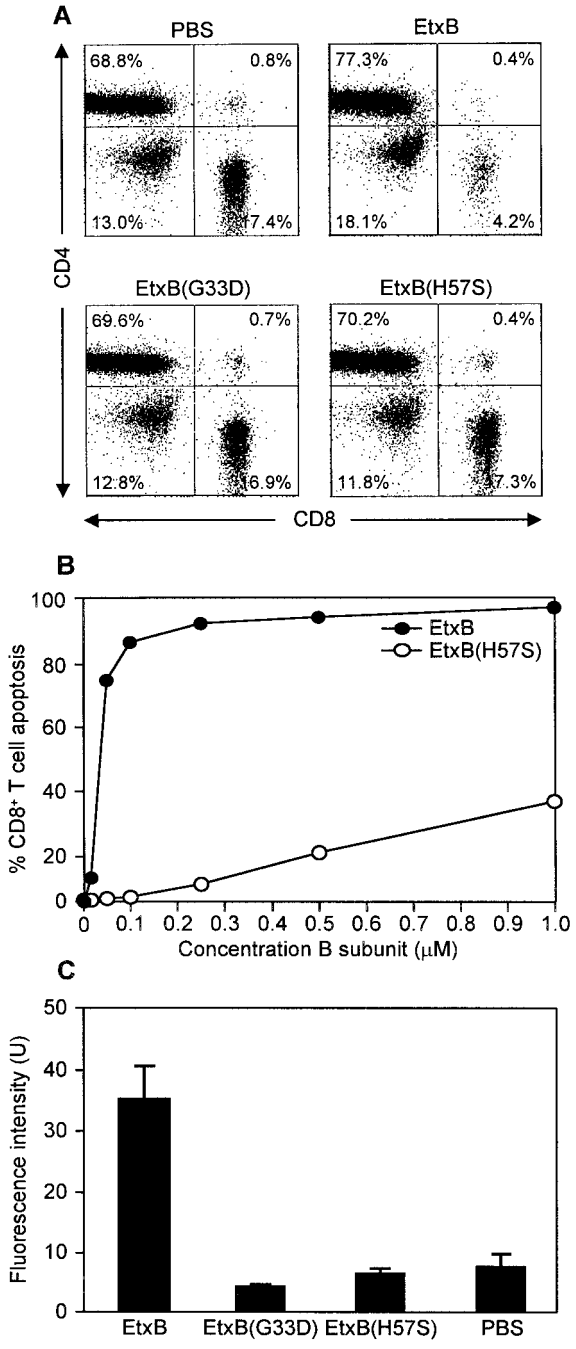

FIG. 3. EtxB(H57S) fails to trigger caspase 3-mediated $CD8^+$ T-cell apoptosis. (A) EtxB(H57S) fails to deplete mixed MLN cell cultures from $CD8^+$ T cells. MLN cells isolated from naive NIH mice were cultured for 48 h in the absence or presence of 100 nM EtxB, EtxB(G33D), or EtxB(H57S) and then stained with both phycoerythrin-labeled CD8-specific and FITC-labeled CD4-specific antibodies. Cells were then analyzed using flow cytometry. The relative percentage of $CD4^+$ T cells, $CD8^+$ T cells, and double-positive and double-negative cells relative to the total MLN population is indicated in each panel. (B) EtxB(H57S) fails to induce $CD8^+$-T-cell apoptosis. MACS-purified $CD8^+$ T cells were cultured as described above with EtxB or EtxB(H57S) at concentrations ranging from 1.5 to 1.0 μM, permeabilized, stained with propidium iodide, and then analyzed using flow cytometry. The percentage of $CD8^+$ T cells in the sub-G_0-G_1 stage of the cell cycle, a characteristic of cells undergoing apoptosis, was calculated and plotted against the concentration of toxin. (C) EtxB(H57S) does not induce caspase 3 activity in $CD8^+$ T-cell lysates. A total of 3×10^6 isolated $CD8^+$ T cells were cultured for 15 h (37°C, 5% CO_2) in the presence of 100 nM EtxB, EtxB(G33D), or EtxB (H57S). Cells were then lysed, the lysates were incubated with the caspase 3 substrate Ac-DEVD-AMC for 30 min, and AMC release was determined using fluorimetry. Cell lysates of $CD8^+$ T cells treated with PBS were used as a negative control. Presented data are representative of two independent experiments.

lack affinity for GM1 (11, 32), did not display a blue shift (Fig. 1C). Moreover, both EtxB and EtxB(H57S), but not EtxB(G33D), were readily detected by a GM1 sandwich ELISA using the EtxB-pentamer-specific MAb LDS16 for detection (Fig. 1E).

Next, we investigated the capacity of EtxB(H57S) to bind to the Jurkat human $CD4^+$-T-cell line and $CD4^+$ and $CD8^+$ T cells isolated from the MLN of naive mice using FACS analysis. T cells were incubated with 100 nM EtxB, EtxB(G33D), or EtxB(H57S) for 1 h on ice, and bound B subunit was then detected using MAb 118-8 and a FITC-labeled secondary antibody and flow cytometry. Figure 2 shows that when $CD8^+$ T cells were incubated with EtxB or EtxB(H57S), a strikingly similar increase in cell fluorescence was detected (compare Fig. 2B and D). In agreement with our previous findings (1, 32), no increase in cell fluorescence was detected when the T cells were incubated with EtxB(G33D) (Fig. 2C). Similar results were obtained with purified $CD4^+$ T cells and Jurkat T cells (Fig. 2E to H and I to L). These results, together with the GM1-ELISA and fluorescence analyses demonstrate that EtxB(H57S) binds to GM1 and to T cells in a fashion similar to that of wild-type EtxB.

EtxB(H57S) fails to trigger caspase 3-mediated apoptosis of $CD8^+$ T cells. To investigate whether EtxB(H57S) retains the in vitro immunomodulatory properties of the wild-type B subunit, we tested whether EtxB(H57S) was capable of inducing apoptosis in $CD8^+$ T cells, a striking example of the modulatory effects of EtxB on lymphocytes (33, 52). Firstly, we assessed the potential of EtxB(H57S) to deplete mixed MLN cell populations of $CD8^+$ T cells. Isolated MLN cells were treated with 100 nM wild-type or mutant B subunit for 48 h, harvested, incubated with fluorescently labeled CD4- and CD8-specific antibodies, and subsequently analyzed by flow cytometry. The relative percentages of $CD4^+$ and $CD8^+$ single-positive, $CD4^+$ $CD8^+$ double-positive, and $CD4^-$ $CD8^-$ double-negative cells were then calculated. Incubation of MLN cells with PBS was used as control. In agreement with our previous findings (33), EtxB strongly depleted mixed MLN cell cultures of $CD8^+$ T cells, without affecting the $CD4^+$-T-cell population (Fig. 3A). By contrast, the nonbinding mutant EtxB(G33D) did not affect either the $CD8^+$- or $CD4^+$-T-cell population (Fig. 3A). Likewise, EtxB(H57S) also failed to deplete MLN cell cultures of $CD8^+$ T cells (Fig. 3A), despite its ability to bind to these cells (Fig. 2D). Consequently, mere cell binding by the B subunits is not sufficient to trigger $CD8^+$ T-cell depletion.

Secondly, we used cell cycle analysis to investigate if the failure of EtxB(H57S) to deplete mixed MLN cell cultures from $CD8^+$ T cells was due to an impaired ability to induce apoptosis. Negatively selected MACS-purified $CD8^+$ T cells were treated with increasing concentrations of EtxB or

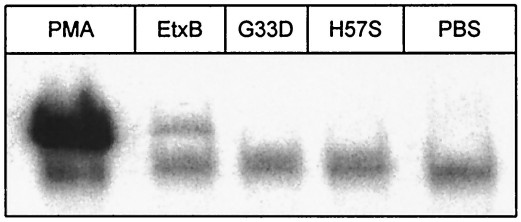

FIG. 4. EtxB(H57S) fails to induce NF-κB activation in Jurkat T cells. Electrophoretic mobility shift assay of nuclear protein extracts from Jurkat T cells cultured in the presence of 100 nM EtxB, EtxB(G33D), or EtxB(H57S) for 2 h are shown. Nuclear protein extracts were prepared as described in Materials and Methods and incubated with a radiolabeled probe containing the consensus sequence of the NF-κB binding site. Binding of NF-κB to the probe was then detected following electrophoresis and autoradiography. In the assay, stimulation of NF-κB activation with PMA (25 ng/ml) or PBS was used as positive or negative control, respectively. No NF-κB binding was detected when nuclear extracts were incubated with a cold unrelated oligonucleotide containing the binding site for AP-1 or with an excess of cold NF-κB oligonucleotide (data not shown). Presented data are representative of two independent experiments.

EtxB(H57S) for 18 h and then washed and permeabilized. Next, propidium iodide was added for DNA staining, and the proportion of cells in the sub-G_0-G_1 stage of the cell cycle, a characteristic of cells undergoing apoptosis, was determined by flow cytometry and plotted against the concentration of B subunit. EtxB, at concentrations as low as 50 nM, induced apoptosis of 75% of the $CD8^+$ T cells. This rose to 82 to 93% apoptosis at EtxB concentrations of 100 nM and higher (Fig. 3B). By contrast, just 2% of $CD8^+$ T cells entered apoptosis when treated with 100 nM EtxB(H57S), and even with 1 μM EtxB(H57S) only 32% of cells underwent apoptosis. Therefore, the failure of EtxB(H57S) to deplete mixed MLN cell cultures of $CD8^+$ T cells appears to be due to an impaired ability to trigger apoptotic pathways.

To assess this more directly, we determined whether EtxB, EtxB(G33D), and EtxB(H57S) activate caspase 3, a key mediator of apoptosis (42). Purified MLN $CD8^+$ T cells were incubated with 100 nM EtxB, EtxB(G33D), or EtxB(H57S) for 15 h, and caspase 3 activity in cell lysates was determined using the artificial caspase 3 substrate Ac-DEVD-AMC as described in Materials and Methods. The treatment of $CD8^+$ T cells with EtxB led to an approximate sixfold increase in caspase 3 activity in cell lysates compared to treatment with PBS (Fig. 3C). Neither EtxB(G33D) nor EtxB(H57S) triggered detectable caspase 3 activation in $CD8^+$ T cells (Fig. 3C).

EtxB(H57S) fails to induce nuclear translocation of NF-κB in Jurkat T cells. Recently, we showed that binding of EtxB to $CD4^+$ and $CD8^+$ T cells triggers signaling events that lead to the nuclear translocation of NF-κB (42). To investigate if binding of EtxB(H57S) leads to the activation of signaling pathways, its capacity to induce nuclear translocation of NF-κB in Jurkat T cells was investigated by band shift analysis. Jurkat T cells were incubated with 100 nM EtxB, EtxB(G33D), or EtxB(H57S) for 3 h, and then nuclear extracts were prepared and incubated with a [γ-^{32}P]ATP-end-labeled oligonucleotide probe containing the binding sequence for NF-κB. Bound NF-κB was then detected by gel electrophoresis followed by autoradiography. Incubation of $CD8^+$ T cells with PMA or PBS was used as positive and negative control, respectively. Figure 4 shows that treatment of Jurkat T cells with PMA resulted in optimal stimulation of nuclear translocation of NF-κB. In agreement with our previous findings on isolated $CD4^+$ and $CD8^+$ T cells (42), EtxB also triggered nuclear translocation of NF-κB in human Jurkat $CD4^+$ T cells (Fig. 4). By contrast, both EtxB(G33D) and EtxB(H57S) failed to stimulate detectable NF-κB DNA-binding activity. These results indicate that EtxB(H57S) lacks the cell-signaling properties of EtxB. This suggests that the His57 residue, or the exposed loop containing this residue, plays a key role in the signaling properties of wild-type EtxB.

EtxB(H57S) lacks immunomodulatory activity in vivo. To investigate whether the defect in the modulation of T cells in vitro correlated with a loss in the immunogenic and adjuvant properties in vivo, mice were immunized intranasally on days 0, 7, and 14 with 10 μg of OVA alone or supplemented with 10 μg of EtxB, EtxB(G33D), or EtxB(H57S). Control animals were given PBS. On day 21 animals were bled and levels of EtxB- and OVA-specific serum IgG were determined by ELISA. Figure 5A shows that EtxB(H57S) failed to stimulate a potent B-subunit-specific serum IgG response. Toxin-specific antibody responses upon immunization with EtxB(H57S) were comparable to those observed upon immunization with the binding mutant EtxB(G33D). Wild-type EtxB, on the other hand, strongly stimulated B-subunit-specific serum IgG responses, resulting in an approximately 350-fold difference in the mean antibody titer upon immunization with EtxB compared to EtxB(H57S). A similar trend was also observed when the mouse sera were examined for OVA-specific serum IgG antibodies (Fig. 5B). Accordingly, compared to immunization with OVA alone, both EtxB(H57S) and EtxB(G33D) failed to stimulate OVA-specific serum IgG responses significantly, whereas coimmunization with EtxB resulted in a significant eightfold enhancement of the OVA-specific serum IgG response. We conclude, therefore, that EtxB(H57S) lacks both the in vitro and in vivo immune stimulatory properties of wild-type EtxB.

EtxB(H57S) retains the ability to traffic and enter the Golgi compartment of Jurkat T cells. The above findings demonstrate that the His57→Ser substitution in EtxB dramatically affects its ability to act as an immunomodulator. The decreased ability of EtxB(H57S) to induce a potent immune response in vivo or to trigger $CD8^+$ T-cell apoptosis or caspase 3 and NF-κB binding activity in vitro implies that the GM1- and cell-binding properties of this molecule cannot be sufficient to activate cell signaling. However, we had not yet investigated if the binding properties of EtxB(H57S) would still enable entry and trafficking into mammalian cells. We therefore decided to investigate cell-binding and entry into Jurkat cells by EtxB(H57S) using confocal microscopy. Jurkat cells were incubated with EtxB, EtxB(G33D), or EtxB(H57S) for 5 or 60 min and then fixed and stained with a polyclonal antiserum specific for EtxB and a FITC-labeled secondary antibody. Furthermore, in order to identify the cellular localization of the B subunits more accurately, fixed cells were treated with TRITC-labeled WGA, specific for *N*-acetyl-β-D-acetylglucosamine present in Golgi-ER and plasma membranes (49).

Figure 6A shows that after 5 min of incubation with B subunit, both EtxB and EtxB(H57S) could be clearly seen at

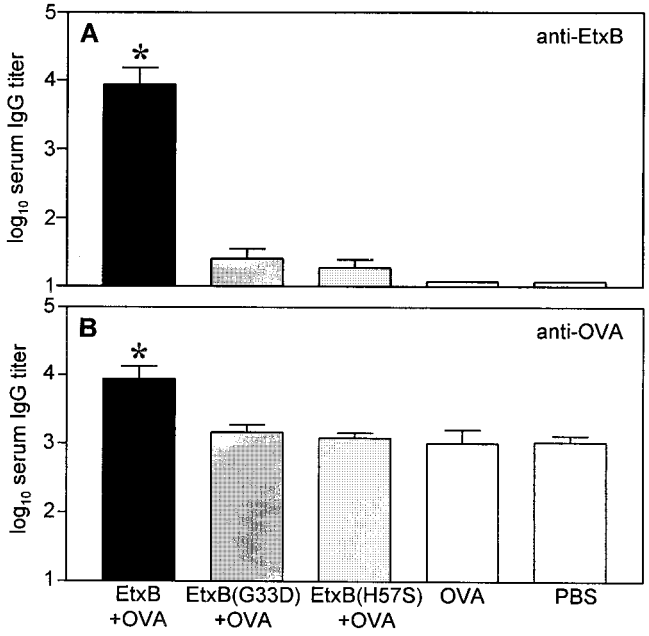

FIG. 5. EtxB(H57S) lacks the immunogenic and adjuvant properties of EtxB in vivo. Groups of eight NIH mice were immunized intranasally under light halothane anesthesia on days 0, 7, and 14 with 10 μg of EtxB, EtxB(G33D), or EtxB(H57A) alone or admixed with 10 μg OVA. Control animals were given PBS. On day 21, animals were bled by cardiac puncture, and EtxB- and OVA-specific serum IgG antibody titers were determined using ELISA as described in Materials and Methods. Titers are given as means + standard deviations (error bars). (A) EtxB-specific serum IgG titers. Differences between groups immunized with EtxB or EtxB(H57S) were statistically significant (*, $P = 0.002$). (B) OVA-specific serum IgG titers. Differences between groups immunized with EtxB plus OVA or OVA alone were statistically significant (*, $P = 0.042$).

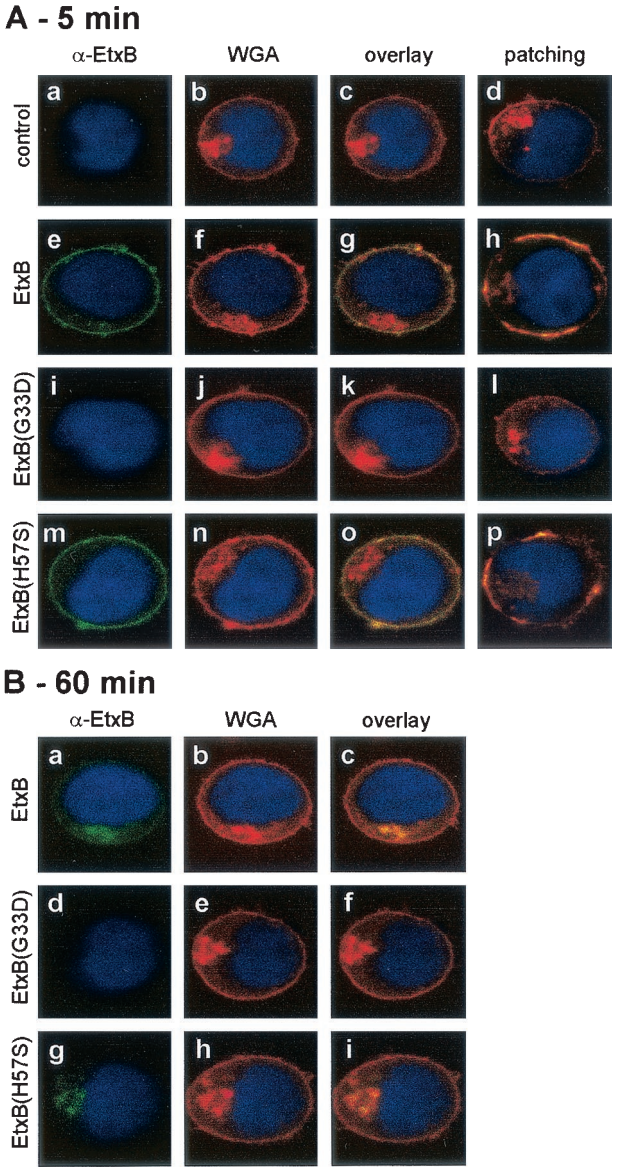

FIG. 6. EtxB(H57S) is capable of entry into Jurkat T cells. Jurkat T cells were incubated with 100 nM EtxB, EtxB(G33D), or EtxB(H57S) for 5 (A) or 60 (B) min at 37°C to demonstrate toxin binding and uptake or were sequentially incubated (30 min, 4°C) with 100 nM EtxB, EtxB(G33D), or EtxB(H57S) and an EtxB-specific polyclonal rabbit antiserum to demonstrate patch formation due to cross-linking of cell-bound toxin. Incubation of Jurkat T cells with PBS was used as a negative control. After toxin treatment, cells were overlaid onto poly-L-lysine coated coverslips, fixed, and permeabilized as described in Materials and Methods. Fixed cells were then incubated with a polyclonal antiserum specific for EtxB, followed by incubation with a FITC-labeled goat antibody specific for mouse IgG, and TRITC-labeled WGA to stain plasma and Golgi membranes. Subsequently, coverslips were mounted on examination slides spotted with Mowiol, which contained DAPI to stain cell nuclei (blue), and then analyzed by confocal microscopy. (A) Panels: a to d, PBS control; e to h, EtxB; i to l, EtxB(G33D); m to p, EtxB(H57S). d, h, l, and p patch formation due to antibody-mediated cross-linking of cell-bound toxin. (B) Panels: a to c, EtxB; d to f, EtxB(G33D); g to i, EtxB(H57S).

the cell surface, and there was almost complete colocalization with the plasma membrane stained with WGA (Fig. 6A, panels e to g and m to o). In addition, with both B subunit preparations there was some indication of cell entry and of colocalization with the Golgi-ER complex (Fig. 6A). When membrane patching was induced by cross-linking cell-surface-bound B subunit using toxin-specific antibodies as described previously (5, 21), it was found that treatment of cells with both EtxB and EtxB(H57S) gave rise to patch formation (Fig. 6A, panels h and p), indicating that these molecules bind to the plasma membrane in a similar fashion. However, with EtxB(G33D) no cell binding, entry, or membrane patching was detected (Fig. 6A, panels i to l).

After 60 min of incubation of Jurkat T cells with the B subunits, both EtxB and EtxB(H57S) were internalized and perinuclear staining was evident, with resultant colocalization with WGA-stained Golgi membranes (Fig. 6B, panels a to c and g to i). Again, no binding or uptake of EtxB(G33D) was detected (Fig. 6B, panels d to f). These results demonstrate that although EtxB(H57S) lacks the ability to induce cell signaling, the His57→Ser mutation does not affect the ability of the molecule to traffic into cells.

EtxB(H57S) can mediate delivery of antigenic peptides into the MHC-I presentation pathway. Recently, we showed that EtxB can be used as a vehicle for the delivery of conjugated

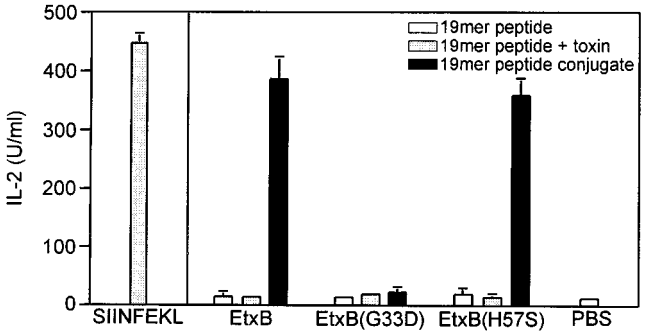

FIG. 7. EtxB(H57S) is capable of delivering a peptide into the MHC-I antigen presentation pathway. EtxB(H57S)-mediated delivery of class I peptides as assessed by analysis of IL-2 release by RF33.70 T-cell hybridoma. JAWSII cells were incubated with 19-mer peptide alone or peptide admixed with or conjugated to EtxB, EtxB(G33D), or EtxB(H57S) at the equivalent concentration of 100 nM peptide for 2 h. Cells were then fixed with 1% paraformaldehyde and incubated overnight with RF33.70 T-cell hybridoma, specific for SIINFEKL peptide in the context of MHC-I. The 8-mer peptide SIINFEKL and PBS were used as positive and negative control, respectively. Duplicate samples were tested, and presented data are given as means + SEM (error bars).

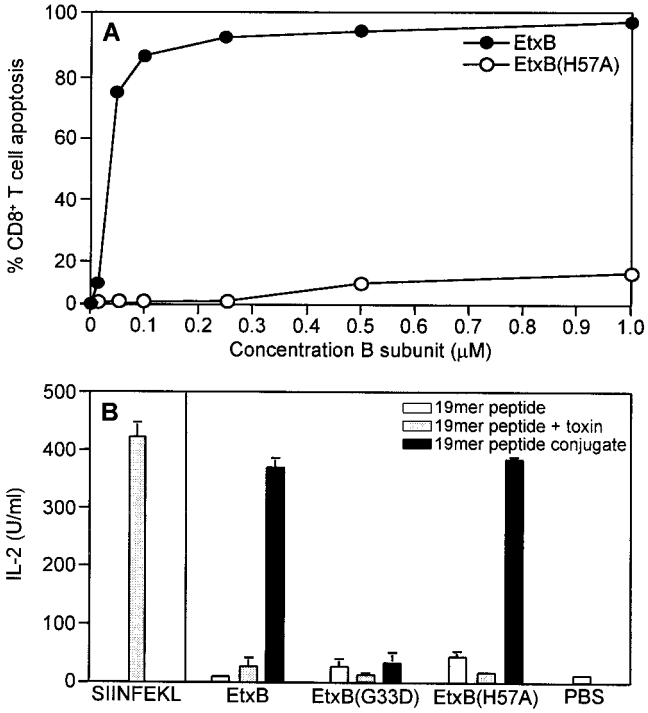

FIG. 8. EtxB(H57A) exhibits similar properties to EtxB(H57S). (A) EtxB(H57A) is severely defective at inducing $CD8^+$-T-cell apoptosis. For details see legend to Fig. 4. (B) EtxB(H57A)-mediated delivery of class I peptides as assessed by analysis of IL-2 release by RF33.70 T-cell-hybridoma. For details see legend to Fig. 7.

peptide epitopes into the MHC-I antigen presentation pathway (9). The ability of EtxB to serve as a vehicle for class I epitope delivery was found to be dependent on the binding of the EtxB-peptide conjugates to GM1 and subsequent entry into acidic endosomes, as well as proteasomal activity. (9). As a result of the above findings on the trafficking of EtxB(H57S) into Jurkat T cells, we speculated that EtxB(H57S) could also be used as an epitope delivery vehicle. To address this, a 19-mer peptide (CAVGAGATAEESIINFEKL), containing an immunodominant MHC-I-restricted epitope from OVA (SIINFEKL), used in our previous study (9), was conjugated to EtxB, EtxB(G33D), and EtxB(H57S) as described in Materials and Methods. The EtxB-, EtxB(G33D)–, and EtxB(H57S)–19-mer conjugates were then assessed for their ability to deliver the SIINFEKL epitope into the MHC-I pathway in a classical antigen presentation assay. In this assay, JAWSII dendritic cells were used as antigen-presenting cells, whereas IL-2 release by RF33.70 T-cell hybridoma, specific for MHC-I/SIINFEKL complexes, was used as an indirect measure of epitope presentation. Incubation of JAWSII cells with the free 8-mer SIINFEKL peptide, which is able to access the MHC-I peptide-binding groove directly by competing for binding with peptides present in already displayed MHC-I complexes, was used as a positive control. Negative controls included 19-mer peptide alone, wild-type and mutant B subunit admixed with 19-mer peptide, and PBS. In all experiments equivalent amounts of either free or conjugated peptide were used.

Figure 7 shows that at a peptide equivalent concentration of 100 nM, both the EtxB–19-mer and EtxB(H57S)–19-mer, but not the EtxB(G33D)–19-mer conjugate efficiently delivered the SIINFEKL epitope into the MHC-I presentation pathway, as evidenced by high-level secretion of IL-2 by the RF33.70 T-cell hybridoma. Furthermore, the observed extent of epitope presentation was similar to that achieved with equivalent amounts of free 8-mer SIINFEKL peptide. Delivery required conjugation to EtxB, as 19-mer peptide alone or admixed with B subunit failed to stimulate presentation. These observations provide definitive evidence that EtxB(H57S) can bind, enter, and deliver attached peptides into cells. This also implies that EtxB(H57S) might be a particularly useful vehicle for facilitating epitope delivery without triggering both an immunomodulatory and potent anti-B-subunit response.

Influence of the amino acid substitution at His57 on the immunomodulatory and trafficking properties of the B subunit. Given that the extent of attenuation in immunomodulatory properties of EtxB may be influenced by the nature of the amino acid substitution at position 57, we chose to investigate if a His→Ala substitution would show any greater or lesser effect on the properties of the molecule. EtxB(H57A), like EtxB(H57S), bound to GM1-coated microtiter plates, exhibited a blue shift in Trp fluorescence upon GM1 addition, and bound to isolated murine $CD4^+$ and $CD8^+$ T cells and Jurkat T cells (data not shown). Upon addition to isolated $CD8^+$ T cells, Etx(H57A) was severely defective at inducing apoptosis and by comparison with EtxB(H57S) was even more attenuated (compare Fig. 8A and 3B). When the CAVGAGATA EESIINFEKL 19-mer peptide was conjugated to EtxB(H57A), peptide delivery and presentation of the SIINFEKL epitope in the context of MHC-I (Fig. 8B) was as efficient as both wild-type EtxB and EtxB(H57S) (compare Fig. 8B and 7). This demonstrates that EtxB(H57A) also retains its trafficking and delivery function but that the nature of the R-group at position 57 can have a subtle but important impact on its immunomodulatory capabilities.

DISCUSSION

In this study we have extensively investigated the properties of a mutant EtxB subunit with a His→Ser substitution at position 57. We show that this substitution results in a striking attenuation in the capacity of the B subunits to act as an immunomodulator and trigger associated signaling events, while at the same time leaving the GM1-binding, cellular uptake, and delivery functions of the molecule intact. These observations have a number of important implications. First, they imply that binding by EtxB to membrane-located GM1 is not sufficient to trigger the signaling events that mediate altered leukocyte differentiation and survival that are thought to be responsible for the potent immunomodulatory properties of the wild-type B subunit. Second, given the similarity in the uptake of EtxB and EtxB(H57S) by Jurkat T cells (Fig. 6), HeLa cells and BHK cells (data not shown), we suggest that the signaling property of the wild-type B subunit, responsible for its immunomodulatory activity, has no impact on the trafficking pathway(s) utilized by EtxB in transiting to the Golgi complex. Third, the loss of immunomodulation, while retaining an ability to deliver attached peptides, means that EtxB(H57S), as well as EtxB(H57A), may prove to be particularly useful class I epitope delivery vehicles since they do not trigger the potent anticarrier response elicited by wild-type EtxB. These findings are consistent with and substantially extend our earlier study on the lack of immunomodulatory activity of CtxB(H57A), a mutant cholera toxin B subunit with a His→Ala substitution at position 57. Taken together, it is evident that the B subunits of both cholera toxin and *E. coli* enterotoxin contain a vital structural element in the His57 loop region that is essential for their profound action on the immune system.

We first investigated the effect of the His→Ser substitution on the GM1- and cell-binding properties of the B subunit. When soluble GM1 was added to either EtxB or EtxB(H57S), the B subunits exhibited a characteristic 12-nm blue shift in fluorescence. It has long been established that the intrinsic fluorescence of EtxB (and CtxB) is due to the sole Trp residue (Trp88) present in each B monomer, which is located close to the interface between the B subunit monomers and forms the floor of the receptor-binding pocket (28). Upon receptor binding, the galactose moiety of GM1 is positioned adjacent to the side chain of Trp88, and this stacking creates a more hydrophobic environment for the indole ring, leading to a blue shift in the emission spectrum of the B subunits (13). Although EtxB and EtxB(H57S) both exhibit a similar blue shift in fluorescence upon GM1 addition, we noted that quenching of the maximum fluorescence intensity was not quite as pronounced for the mutant B subunit. This could be to due to subtle alterations in the electrostatic environment or solvent exposure of Trp88 as a result of the altered position of the exposed loop or to the change in the R-group with the His→Ser substitution. Nevertheless, both wild-type EtxB and EtxB(H57S) exhibit indistinguishable binding curves in GM1-ELISAs, consistent with the view that the two molecules have very similar GM1-binding modes. The observation that EtxB(H57S), but not EtxB(G33D), also binds to isolated $CD8^+$ and $CD4^+$ T cells and to Jurkat T cells in amounts comparable to wild-type EtxB, and that both EtxB and EtxB(H57S) traffic to a similar extent into the Golgi network, lend further support to the conclusion that EtxB(H57S) retains its lectin-binding activity.

Despite their similarities, EtxB(H57S) differs markedly from wild-type EtxB in affecting leukocyte differentiation and survival, as evidenced by a marked reduction in $CD8^+$ T-cell apoptosis, an inability to up-regulate MHC-II expression on B cells (S. A. Fraser and T. R. Hirst, unpublished observation), and a failure to activate NF-κB in Jurkat T cells. This also correlated with a corresponding reduction in in vivo immunogenicity and a lack of adjuvant activity. Thus, while EtxB (H57S) still binds (and enters) leukocytes, it is unable to activate the signaling cascades that makes EtxB and CtxB such potent modulators of mammalian immune systems.

These findings make it increasingly implausible that GM1 binding alone is the sole trigger for B-subunit-mediated cell signaling. This might be interpreted in a number of ways. Firstly, it is possible that the signaling capabilities of EtxB and CtxB rely on binding to alternative receptors other than GM1. Early studies by Fishman and coworkers provided evidence that GM1 is the functional receptor for toxin action, at least as far as triggering an elevation in cyclic AMP levels is concerned (15, 35). However, those studies would not have identified if interaction with other receptors might trigger B subunit-mediated effects. It is known that, in addition to its affinity for GM1, EtxB also has the ability to bind to GD1b, asialo GM1, GM2, and a variety of galactose-containing glycolipids and galactoproteins (17, 20, 34, 50). The significance of these alternative receptors has remained speculative, with some evidence that they may allow GM1-independent entry of the toxin into the diarrheagenic pathway (20). It is conceivable that one or a combination of these alternative receptors might be responsible for triggering B subunit-mediated immunomodulation. If so, then CtxB would also need to be able to bind to the same alternative receptors, thus excluding most of the alternative EtxB receptors to which CtxB shows no affinity. GD1b is an alternative receptor to which both CtxB and EtxB bind with a K_d approximately 10-fold lower than that for GM1 (22, 26). Interestingly, in a GD1b-ELISA we found that EtxB(H57S) and EtxB(H57A) both bound poorly to GD1b compared to EtxB (Fraser and Hirst, unpublished observations). However, when the GD1b binding sites on $CD8^+$ T cells were blocked by preincubation with tetanus toxin C fragment, or when $CD8^+$ T cells were pretreated with *V. cholerae* neuraminidase, which converts GD1b into GM1 (3), no significant effect on EtxB-mediated $CD8^+$-T-cell apoptosis was observed (Fraser and Hirst, unpublished observations). This suggests that GD1b is not the receptor involved in immunomodulation.

Another explanation would be that when the B subunits bind to GM1 they are strategically positioned at the membrane surface to interact with other membrane components, possibly constituting a coreceptor, that are involved in mediating cell signaling. It is conceivable that after binding to GM1, the loops in the B pentamer are positioned to directly interact with, for example, a glucosylphosphatidylinositol-anchored or transmembrane protein. The alteration in the position of the loops in the His57 mutants may prevent this from happening, even though the molecule is tethered to the membrane via GM1. Importantly, GM1 is preferentially located in cholesterol-rich detergent-insoluble membrane microdomains or lipid rafts, which contain numerous proteins involved in cell signaling (21,

57). If CtxB- and EtxB-GM1 complexes do indeed interact with additional membrane proteins in leukocytes, its identity might offer new insights into the mechanisms controlling immune responsiveness.

It has recently been proposed that toxin binding to GM1 represents a form of protein-lipid modification that provides a sorting motif for association with lipid rafts and retrograde trafficking into the secretory pathway of mammalian cells (23, 57). Here, we show that the His57 mutants exhibit normal trafficking properties, and are able to gain access to this pathway. This contrasts with our earlier reports on the properties of a holotoxin-derivative of Ctx, which contained a wild-type A subunit complexed with CtxB(H57A). This mutant holotoxin lacked enterotoxic properties when applied to polarized human intestinal T84 cells (1, 39) and appeared to bind less stably to T84 cells than wild-type Ctx (39). The explanation for this discrepancy remains unclear, but it may stem from the differences in the cell types investigated. For example, the organization of GM1 in the apical membrane of polarized epithelial cells may be different, since other glycolipids such as GD1a partition into detergent-soluble fractions in T84 cells but are in the detergent insoluble fraction in other cell types (57). It is also conceivable that the putative signaling coreceptor may be absent from T84 cells, thus influencing the avidity of the mutant B subunits for the membrane surface. In this regard, we have been unable to detect any CtxB- or EtxB-mediated activation events in T84 cells, such as modulation in cytokine production, that normally occur when the B subunits are added to leukocytes (45, 53). The efficient uptake of EtxB(H57S) and EtxB(H57A) by Jurkat T cells, in the absence of apparent cell signaling, underscores the view that interaction with additional molecules and any associated activation of signaling cascades plays no role in toxin uptake.

The finding that EtxB(H57S) and EtxB(H57A) could traffic into Jurkat T cells led us to test the possibility that these mutants might be useful as delivery vehicles for antigenic peptides. Previously, we had shown that wild-type EtxB could be used to deliver attached class I epitopes into the endogenous MHC-I antigen presentation pathway (9). Here, we show that EtxB(H57S) and EtxB(H57A) are as effective as wild-type EtxB in delivering a model class I epitope using this system. The similarity in efficacy between mutant and wild-type B subunits means that the substitution of His57 has no adverse affect on B subunit binding or uptake, or on epitope release and presentation. Given that the mutants do not stimulate a potent anticarrier response, it is conceivable they might be more useful delivery vehicles than wild-type EtxB. Moreover, one of the immunomodulatory properties of wild-type EtxB is to induce IL-10 and inhibit IL-12 production by monocytes, thereby creating a cytokine environment favoring Th2 rather than Th1 responses (7, 53). It is now recognized that Th1 cells may provide more effective help for the development and maintenance of cytotoxic-T-lymphocyte responses (18). Thus, the H57 mutants, which do not trigger $CD8^+$-T-cell apoptosis or induce the cell-signaling cascades responsible for biasing towards a Th2 response, could offer a more-effective means of inducing MHC-I-restricted cytotoxic-T-lymphocyte responses following their use as delivery vehicles for class I epitopes.

In conclusion, the H57 mutants represent novel tools for investigating the complex cellular interactions and signaling events occurring after receptor binding, as well as offering an alternative means of delivering attached peptides in the absence of the potent immunomodulatory signals induced by the wild-type B subunits.

ACKNOWLEDGMENTS

We thank Karen Reynard and Helen Webb for construction of plasmids and Tamera Jones and Martin Kenny for assistance in purifying EtxB and EtxB(G33D). We thank Mark Jepson for guidance in the use of confocal microscopy and Sigmar Leyer for establishing conditions for optimal EtxB-peptide conjugation. We thank Wayne Lencer for critically reading the manuscript.

S.A.F. and A.R.H. were recipients of Medical Research Council studentships. This work was supported by grant G9818467 from the Medical Research Council of the United Kingdom. We thank the Medical Research Council for providing an Infrastructure Award and Joint Research Equipment Initiative Grant to establish the School of Medical Sciences Cell Imaging Facility.

REFERENCES

1. **Aman, A. T., S. Fraser, E. A. Merritt, C. Rodigherio, M. Kenny, M. Ahn, W. G. J. Hol, N. A. Williams, W. I. Lencer, and T. R. Hirst.** 2001. A mutant cholera toxin B subunit that binds GM1-ganglioside but lacks immunomodulatory or toxic activity. Proc. Natl. Acad. Sci. USA **98:**8536–8541.
2. **Amin, T., and T. R. Hirst.** 1994. Purification of the B-subunit oligomer of *Escherichia coli* heat-labile enterotoxin by heterologous expression and secretion in a marine *Vibrio*. Protein Expr. Purif. **5:**198–204.
3. **Barton, N. W., and A. Rosenberg.** 1973. Action of *Vibrio cholerae* neuraminidase (sialidase) upon the surface of intact cells and their isolated sialolipid components. J. Biol. Chem. **248:**7353–7358.
4. **Bergerot, I., C. Ploix, J. Petersen, V. Moulin, C. Rask, N. Fabien, M. Lindblad, A. Mayer, C. Czerkinsky, J. Holmgren, and C. Thivolet.** 1997. A cholera toxoid-insulin conjugate as an oral vaccine against spontaneous autoimmune diabetes. Proc. Natl. Acad. Sci. USA **94:**4610–4614.
5. **Bone, H., S. Eckholdt, and N. A. Williams.** 2002. Modulation of B lymphocyte signalling by the B subunit of *Escherichia coli* heat-labile enterotoxin. Int. Immunol. **14:**647–658.
6. **Bone, H., and N. A. Williams.** 2001. Antigen-receptor cross-linking and lipopolysaccharide trigger distinct phosphoinositide 3-kinase-dependent pathways to NF-kappa B activation in primary B cells. Int. Immunol. **13:** 807–816.
7. **Braun, M. C., J. He, C. Y. Wu, and B. L. Kelsall.** 1999. Cholera toxin suppresses interleukin (IL)-12 production and IL-12 receptor β1 and β2 chain expression. J. Exp. Med. **189:**541–552.
8. **Bromander, A., J. Holmgren, and N. Lycke.** 1991. Cholera toxin stimulates IL-1 production and enhances antigen presentation by macrophages *in vitro*. J. Immunol. **146:**2908–2914.
9. **De Haan, L., A. R. Hearn, A. J. Rivett, and T. R. Hirst.** 2002. Enhanced delivery of exogenous peptides into the class I antigen processing and presentation pathway. Infect. Immun. **70:**3249–3258.
10. **De Haan, L., and T. R. Hirst.** 2000. Cholera toxin and related enterotoxins: a cell biological and immunological perspective. J. Nat. Toxins **9:**281–297.
11. **De Haan, L., W. R. Verweij, I. K. Feil, M. Holtrop, W. G. J. Hol, E. Agsteribbe, and J. Wilschut.** 1998. Role of GM1-binding in the mucosal immunogenicity and adjuvant activity of the *Escherichia coli* heat-labile enterotoxin and its B subunit. Immunology. **94:**424–430.
12. **De Haan, L., W. R. Verweij, I. K. Feil, T. H. Lijnema, W. G. J. Hol, E. Agsteribbe, and J. Wilschut.** 1996. Mutants of the *Escherichia coli* heat-labile enterotoxin with reduced ADP-ribosylation activity or no activity retain the immunogenic properties of the native holotoxin. Infect. Immun. **64:**5413–5416.
13. **De Wolf, M. J. S., M. Fridkin, and L. D. Kohn.** 1981. Tryptophan residues of cholera toxin and its A and B protomers. Intrinsic fluorescence and solute quenching upon interacting with the ganglioside GM1, oligo-GM1, or dansylated oligo-GM1. J. Biol. Chem. **256:**5489–5496.
14. **Elson, C. O., and W. Ealding.** 1984. Generalized systemic and mucosal immunity in mice after mucosal stimulation with cholera toxin. J. Immunol. **132:**2736–2741.
15. **Fishman, P. H., and E. E. Atikkan.** 1980. Mechanism of action of cholera toxin: effect of receptor density and multivalent binding on activation of adenylate cyclase. J. Membr. Biol. **54:**51–60.
16. **Francis, M. L., J. Ryan, M. G. Jobling, R. K. Holmes, J. Moss, and J. J. Mond.** 1992. Cyclic AMP-independent effects of cholera toxin on B cell activation. II: binding of GM1 induces B cell activation. J. Immunol. **148:** 1999–2005.
17. **Fukuta, S., J. L. Magnani, E. M. Twiddy, R. K. Holmes, and V. Ginsburg.** 1988. Comparison of the carbohydrate-binding specificities of cholera toxin

and *Escherichia coli* heat-labile enterotoxins LTh-I, LT-IIa, and LT-IIb. Infect. Immun. **56:**1748–1753.
18. **Hasenkrug, K. J., and U. Dittmer.** 2000. The role of CD4 and CD8 T cells in recovery and protection from retroviral infection: lessons from the Friend virus model. Virology **272:**244–249.
19. **Higuchi, R., B. Krummel, and R. K. Saiki.** 1988. A general method of *in vitro* preparation and specific mutagenesis of DNA fragments: study of protein and DNA interactions. Nucleic Acids Res. **16:**7351–7367.
20. **Holmgren, J., P. Fredman, M. Lindblad, A.-M. Svennerholm, and L. Svennerholm.** 1982. Rabbit intestinal glycoprotein receptor for *Escherichia coli* heat-labile enterotoxin lacking affinity for cholera toxin. Infect. Immun. **38:**424–433.
21. **Janes, P. W., S. C. Ley, and A. I. Magee.** 1999. Aggregation of lipid rafts accompanies signaling via the T cell antigen receptor. J. Cell Biol. **147:**447–461.
22. **Kuziemko, G. M., M. Stroh, and R. C. Stevens.** 1996. Cholera toxin binding affinity and specificity for gangliosides determined by surface plasmon resonance. Biochemistry **35:**6375–6384.
23. **Lencer, W. I., T. R. Hirst, and R. K. Holmes.** 1999. Membrane traffic and the cellular uptake of cholera toxin. Biochim. Biophys. Acta **1450:**177–190.
24. **Lycke, N., A. K. Bromander, L. Ekman, U. Karlsson, and J. Holmgren.** 1989. Cellular basis of immunomodulation by cholera toxin *in vitro* with possible association to the adjuvant action *in vivo*. J. Immunol. **142:**20–27.
25. **Lycke, N., and J. Holmgren.** 1986. Strong adjuvant properties of cholera toxin on gut mucosal immune responses to orally presented antigens. Immunology **59:**301–308.
26. **MacKenzie, C. R., T. Hirama, K. K. Lee, E. Altman, and N. M. Young.** 1997. Quantitative analysis of bacterial toxin affinity and specificity for glycolipid receptors by surface plasmon resonance. J. Biol. Chem. **272:**5533–5538.
27. **Matousek, M. P., J. G. Nedrud, and C. V. Harding.** 1996. Distinct effects of recombinant cholera toxin B subunit and holotoxin on different stages of class II MHC antigen processing and presentation by macrophages. J. Immunol. **156:**4137–4145.
28. **Merritt, E. A., T. K. Sixma, K. H. Kalk, B. A. M. Van Zanten, and W. G. J. Hol.** 1994. Galactose-binding site in *Escherichia coli* heat-labile enterotoxin (LT) and cholera toxin (CT). Mol. Microbiol. **13:**745–753.
29. **Millar, D. G., and T. R. Hirst.** 2001. Cholera toxin and *Escherichia coli* enterotoxin B-subunits inhibit macrophage-mediated antigen processing and presentation: evidence for antigen persistence in non-acidic recycling endosomal compartments. Cell. Microbiol. **3:**311–329.
30. **Millar, D. G., T. R. Hirst, and D. P. Snider.** 2001. *Escherichia coli* heat-labile enterotoxin B subunit is a more potent mucosal adjuvant than its closely related homologue, the B subunit of cholera toxin. Infect. Immun. **69:**3476–3482.
31. **Nashar, T. O., T. R. Hirst, and N. A. Williams.** 1997. Modulation of B-cell activation by the B subunit of *Escherichia coli* enterotoxin: receptor interaction up-regulates MHC class II, B7, CD40, CD25 and ICAM-1. Immunology **91:**572–578.
32. **Nashar, T. O., H. M. Webb, S. Eaglestone, N. A. Williams, and T. R. Hirst.** 1996. Potent immunogenicity of the B subunits of *Escherichia coli* heat-labile enterotoxin: Receptor binding is essential and induces differential modulation of lymphocyte subsets. Proc. Natl. Acad. Sci. USA **93:**226–230.
33. **Nashar, T. O., N. A. Williams, and T. R. Hirst.** 1996. Cross-linking of cell surface ganglioside GM1 induces the selective apoptosis of mature CD8+ T lymphocytes. Int. Immunol. **8:**731–736.
34. **Orlandi, P. A., D. R. Critchley, and P. H. Fishman.** 1994. The heat-labile enterotoxin of *Escherichia coli* binds to polylactosaminoglycan-containing receptors in CaCo-2 human intestinal epithelial cells. Biochemistry **33:**12886–12895.
35. **Pacuszka, T., R. M. Bradley, and P. H. Fishman.** 1991. Neoglycolipid analogues of ganglioside GM1 as functional receptors of cholera toxin. Biochemistry **30:**2563–2570.
36. **Rappuoli, R., M. Pizza, G. Douce, and G. Dougan.** 1999. Structure and mucosal adjuvanticity of cholera and *Escherichia coli* heat-labile enterotoxins. Immunol. Today **20:**493–500.
37. **Richards, C. M., A. T. Aman, T. R. Hirst, T. J. Hill, and N. A. Williams.** 2001. Protective mucosal immunity to ocular herpes simplex virus type 1 infection in mice by using *Escherichia coli* heat-labile enterotoxin B subunit as an adjuvant. J. Virol. **75:**1664–1671.
38. **Rock, K. L., L. Rothstein, and S. Gamble.** 1990. Generation of class I MHC-restricted T-T hybridomas. J. Immunol. **145:**804–811.
39. **Rodighiero, C., Y. Fujinaga, T. R. Hirst, and W. I. Lencer.** 2001. A cholera toxin B-subunit variant that binds ganglioside GM1 but fails to induce toxicity. J. Biol. Chem. **276:**36939–36945.
40. **Ruddock, L. W., S. P. Ruston, S. M. Kelly, N. C. Price, R. B. Freedman, and T. R. Hirst.** 1995. Kinetics of acid-mediated disassembly of the B subunit pentamer of *Escherichia coli* heat-labile enterotoxin. Molecular basis of pH stability. J. Biol. Chem. **270:**29953–29958.
41. **Ruddock, L. W., H. M. Webb, S. P. Ruston, C. Cheesman, R. B. Freedman, and T. R. Hirst.** 1996. A pH-dependent conformational change in the B-subunit pentamer of *Escherichia coli* heat-labile enterotoxin: structural basis and possible functional role for a conserved feature of the AB(5) toxin family. Biochemistry **35:**16069–16076.
42. **Salmond, R. J., R. S. Pitman, E. Jimi, M. Soriani, T. R. Hirst, S. Ghosh, M. Rincon, and N. A. Williams.** 2002. CD8+ T cell apoptosis induced by *Escherichia coli* heat-labile enterotoxin B subunit occurs via a novel pathway involving NF-κB-dependent caspase activation. Eur. J. Immunol. **32:**1737–1747.
43. **Schneider, U., H. U. Schwenk, and G. Bornkamm.** 1977. Characterization of EBV-genome negative "null" and "T" cell lines derived from children with acute lymphoblastic leukemia and leukemic transformed non-Hodgkin lymphoma. Int. J. Cancer **19:**621–626.
44. **Sears, C. L., and J. B. Kaper.** 1996. Enteric bacterial toxins: mechanisms of action and linkage to intestinal secretion. Microbiol. Rev. **60:**167–215.
45. **Soriani, M., L. Bailey, and T. R. Hirst.** 2002. Contribution of the ADP-ribosylating and receptor-binding properties of cholera-like enterotoxins in modulating cytokine secretion by human intestinal epithelial cells. Microbiology **148:**667–676.
46. **Soriani, M., N. A. Williams, and T. R. Hirst.** 2001. *Escherichia coli* enterotoxin B subunit triggers apoptosis of CD8+ T cells by activating transcription factor c-Myc. Infect. Immun. **69:**4923–4930.
47. **Spangler, B. D.** 1992. Structure and function of cholera toxin and the related *Escherichia coli* heat-labile enterotoxin. Microbiol. Rev. **56:**622–647.
48. **Sun, J. B., C. Rask, T. Olsson, J. Holmgren, and C. Czerkinsky.** 1996. Treatment of experimental autoimmune encephalomyelitis by feeding myelin basic protein conjugated to cholera toxin B subunit. Proc. Natl. Acad. Sci. USA **93:**7196–7201.
49. **Tartakoff, A. M., and P. Vassalli.** 1983. Lectin-binding sites as markers of Golgi subcompartments: proximal-to-distal maturation of oligosaccharides. J. Cell Biol. **97:**1243–1248.
50. **Teneberg, S., T. R. Hirst, J. Angstrom, and K. A. Karlsson.** 1994. Comparison of the glycolipid-binding specificities of cholera toxin and porcine *Escherichia coli* heat-labile enterotoxin: identification of a receptor-active non-ganglioside glycolipid for the heat-labile toxin in infant rabbit small intestine. Glycoconj. J. **11:**533–540.
51. **Tochikubo, K., M. Isaka, Y. Yasuda, S. Kozuka, K. Matano, Y. Miura, and T. Taniguchi.** 1998. Recombinant cholera toxin B subunit acts as an adjuvant for the mucosal and systemic responses of mice to mucosally co-administered bovine serum albumin. Vaccine **16:**150–155.
52. **Truitt, R. L., C. Hanke, J. Radke, R. Mueller, and J. T. Barbieri.** 1998. Glycosphingolipids as novel targets for T-cell suppression by the B subunit of recombinant heat-labile enterotoxin. Infect. Immun. **66:**1299–1308.
53. **Turcanu, V., T. R. Hirst, and N. A. Williams.** 2002. Modulation of human monocytes by *Escherichia coli* heat-labile enterotoxin B-subunit; altered cytokine production and its functional consequences. Immunology **106:**316–325.
54. **Verweij, W. R., L. de Haan, M. Holtrop, R. Brands, G. J. M. van Scharrenburg, E. Agsteribbe, and J. Wilschut.** 1998. Mucosal immunoadjuvant activity of the recombinant *Escherichia coli* heat-labile enterotoxin and its B subunit: Induction of systemic IgG and secretory IgA responses in mice by intranasal immunization with influenza surface antigen. Vaccine **16:**2069–2076.
55. **Williams, N. A., T. R. Hirst, and T. O. Nashar.** 1999. Immune modulation by the cholera-like enterotoxins: from adjuvant to therapeutic. Immunol. Today **20:**95–101.
56. **Williams, N. A., L. M. Stasiuk, T. O. Nashar, C. M. Richards, A. K. Lang, M. J. Day, and T. R. Hirst.** 1997. Prevention of autoimmune disease due to lymphocyte modulation by the B-subunit of *Escherichia coli* heat-labile enterotoxin. Proc. Natl. Acad. Sci. USA **94:**5290–5295.
57. **Wolf, A. A., M. G. Jobling, S. Wimer Mackin, M. Ferguson Maltzman, J. L. Madara, R. K. Holmes, and W. I. Lencer.** 1998. Ganglioside structure dictates signal transduction by cholera toxin and association with caveolae-like membrane domains in polarized epithelia. J. Cell Biol. **141:**917–927.
58. **Woogen, S. D., W. Ealding, and C. O. Elson.** 1987. Inhibition of murine lymphocyte proliferation by the B subunit of cholera toxin. J. Immunol. **139:**3764–3770.
59. **Wu, H. Y., and M. W. Russell.** 1998. Induction of mucosal and systemic immune responses by intranasal immunization using recombinant cholera toxin B subunit as an adjuvant. Vaccine **16:**286–292.
60. **Yankelevich, B., V. A. Soldatenkov, J. Hodgson, A. J. Polotsky, K. Creswell, and A. Mazumder.** 1996. Differential induction of programmed cell death in CD8+ and CD4+ T cells by the B subunit of cholera toxin. Cell. Immunol. **168:**229–234.
61. **Yu, J., H. Webb, and T. R. Hirst.** 1992. A homologue of the *Escherichia coli* DsbA protein involved in disulphide bond formation is required for enterotoxin biogenesis in Vibrio cholerae. Mol. Microbiol. **6:**1949–1958.

Editor: J. T. Barbieri